8.3 MULTI-DOPPLER RADAR ANALYSIS OF A TORNADIC THUNDERSTORM USING A 3D VARIATIONAL DATA ASSIMILATION TECHNIQUE AND ARPS MODEL

Edward Natenberg and Jidong Gao
School of Meteorology and Center for Analysis and Prediction of Storms
University of Oklahoma, Norman, OK

1. INTRODUCTION

Several methods have been successfully used to analyze and assimilate radar observations into a numerical weather prediction (NWP) model including a four dimensional variational method (Sun and Crook 1997, 1998), a single Doppler velocity retrieval method developed by Weygant et al. (2002), a three dimensional variational method (3DVAR) (Gao et al. 2001; Gao et al. 2004; Hu et al. 2006a, b) and an ensemble Kalman filter method (Dowell et al. 2004; Wicker et al. 2004). These methods usually include retrieving the three dimensional wind field as well as the thermodynamic and microphysical parameters from radar because radar can observe only radial velocity and reflectivity.

Most of the previous research about radar data assimilation only used observations from one or two radars located close to the convection being studied, therefore limiting the information available to provide a complete set of initial conditions, and which did not take full advantage of WSR-88D radar network. By only using data from one, or two nearby radars in an analysis, only a small portion of the atmosphere is observed, and a large part of atmosphere can not be effectively observed due to the cone of silence located above the radar. When including several additional radars located father away from targeted convection, such as a tornadic thunderstorm, it is possible that the upper portions of the atmosphere could also be observed giving a complete picture of the current atmospheric state.

The impact of using the WSR-88D radar network to perform a variational analysis and storm scale forecast is explored in this study using radar data from a supercell on 8 May 2003 in central Oklahoma. The storm spawned a F4 tornado that tracked through southern Oklahoma City causing $370 million in damage and 134 injuries. By using data from up to five radars (including four WSR-88Ds and one TDWR), velocity and reflectivity measurements at both the low-level and upper levels of a thunderstorm can be observed. This increases the accuracy of the estimated, or retrieved, wind and thermodynamic variables, when compared to an analysis using data from only single radar.

Corresponding author address: Edward Natenberg, Univ. of Oklahoma, School of Meteorology, NWC Suite 5900, 120 David Boren Blvd, Norman, OK, 73072; eddienatenberg@ou.edu

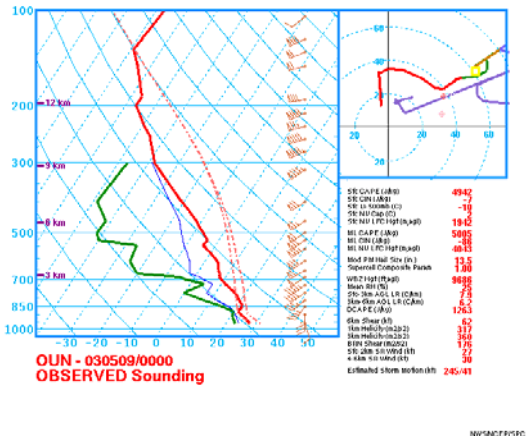

Fig. 1. 0000 UTC 8 May 2003 sounding from Norman, OK.

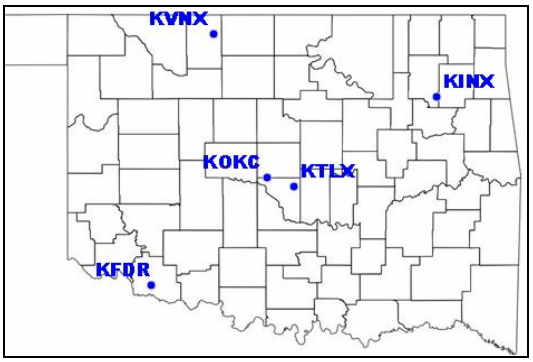

Fig. 2. The location of the four (KTLX, KVNX, KFDR, KINX) WSR-88D and one TDWR (KOKC) radars observing the atmosphere over central Oklahoma.

2. THE MAY 8 TORNADIC STORM and 1-KM ANALYSIS DESIGN

The 8 May 2003 tornadic thunderstorm formed in a very unstable environment characterized by large values of CAPE (4942 J kg^{-1}), very low CIN (-7 J kg^{-1}), and high amounts of low level helicity (360 m^2s^{-2}) (Shown in Fig. 1). An approaching shortwave trough and surface based dryline helped to initiate isolated convection in central Oklahoma by 2100 UTC which tracked into the Oklahoma City area by 2200 UTC.

The analyses were performed using the Advanced Regional Prediction System (ARPS) 3DVAR analysis package with a horizontal grid resolution of 1-km and an average vertical resolution of 500-m. In the vertical, the use of grid stretching was employed based on a cubic function with a minimum resolution of 100-m. The domain size was 157 x 143 x 47 grid points with the center of the domain located just south of Del City, Oklahoma, east-southeast of Oklahoma City, at the location where spotters reported a large tornado. An analysis was performed every 5 minutes beginning from 2145 until 2240 UTC.

The background field was obtained from the operational ETA model, which was interpolated from a coarser grid resolution of 40-km to a 9-km grid for use in a forecast using only sounding data starting from 1800 UTC. This forecast was then used as the background for the analysis. Apart from radar data, the observational data used in this study also include Oklahoma Climate Survey (OCS) Mesonet observations, upper air soundings, and profiler data. Mesonet observations for each analysis were updated every five minutes to coincide with the analysis times. The radar data used in this study consisted of four, WSR-88D operational NWS radars, KINX, KVNX, KTLX, KFDR, and one terminal Doppler weather radar (TDWR), KOKC, operated by Will Rogers Airport in Oklahoma City (Shown in Fig. 2). Since radar observations were obtained at different times, scans closest (either before or after) to the time of the analysis were used. A complex cloud analysis package was used to adjust values of the cloud water, rain water, and water vapor mixing ratios based on reflectivity data. No potential temperature adjustments were done to account for latent heat. This helped to avoid overestimating thermodynamic instability within the model since the background already included large values of CAPE through a significant portion of the atmosphere.

3. IMPACT OF THE USE OF MULTIPLE RADARS IN THE 1-KM ANALYSIS

Two analyses were performed, one control run using all five available radars, and one analysis only using data from the KOKC radar. In both analyses surface data and upper air data was used. The control experiment in Fig. 3 shows a right split and a left split thunderstorm located just east of the dryline at (a) 2145 UTC and continues to develop into a mature supercell by (b) 2200 UTC when a hook echo structure is most apparent.

When performing an analysis using radars close to the thunderstorm, areas directly above the radars can not be observed due to the cone of silence. However, radars located far from the thunderstorm could observe the structure above the 3-km AGL due to the increase of the altitude of each observation with increasing distance from the radar. This is evident in Fig. 4 where large chunks of reflectivity data are missing above the 8-km AGL in Fig. 4b, when compared to Fig. 4a.

This area of missing information in the KOKC radar analysis is replaced with information from the background field and upper air observations which are poor estimates of analyzed fields in areas of deep convection. The impact of this is most noticeable in the divergent structure above the updraft at the 12-km AGL (Fig. 5).

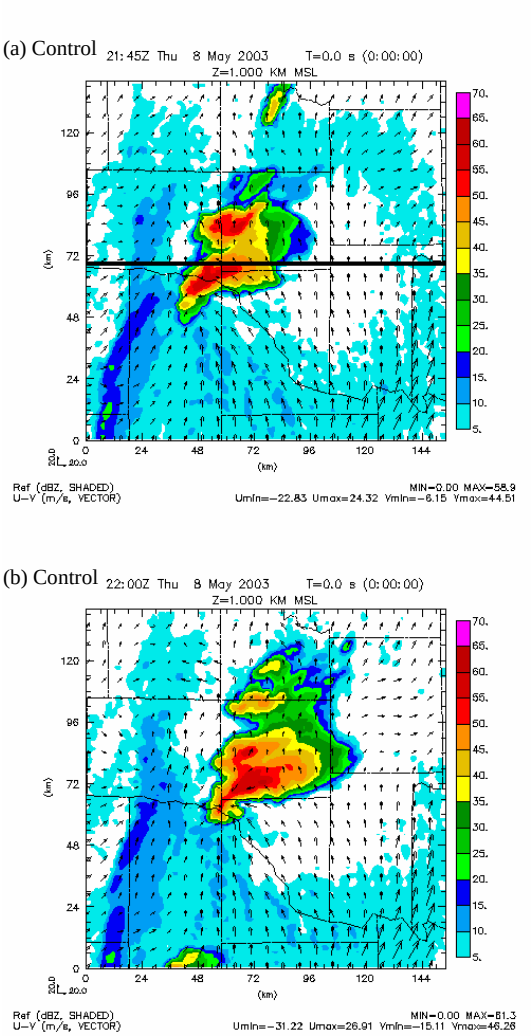

Fig. 3. Control analysis 1-km reflectivity using data from five radars at (a) 2145 UTC and (b) 2200 UTC. The black line denotes the location of the cross section in Fig. 3.

A second aspect of using data from only one radar is the cross beam component of the wind which cannot be observed. Poor estimates in the cross beam component of the wind in the analysis were most noticeable at 2200 UTC along the front flank of the thunderstorm at the 1-km AGL just east of the mesocyclone. The underestimated magnitude of the wind in this region con-

tributed to values of negative vorticity just northeast of the mesocyclone shown in Fig. 6. At higher levels in the atmosphere the vorticity structure was still improved in the control run when compared to the one radar (KOKC) analysis. Fig. 6a clearly shows the cyclonic and anticyclonic dipole structure described by Rotunno (1981) and simulated by Wilhelmson and Klemp (1978). This structure shows that the supercell features in this case are best resolved using data from multiple radars, which can avoid the underdetermined problems that are associated with the cross beam component of the wind and cannot be well estimated due to the lack of radar coverage.

(a) Control

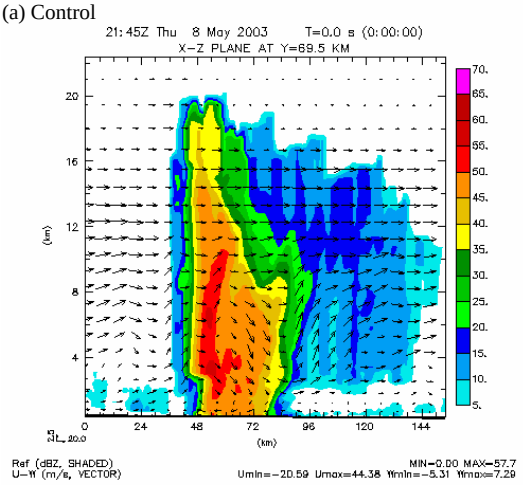

(b) KOKC

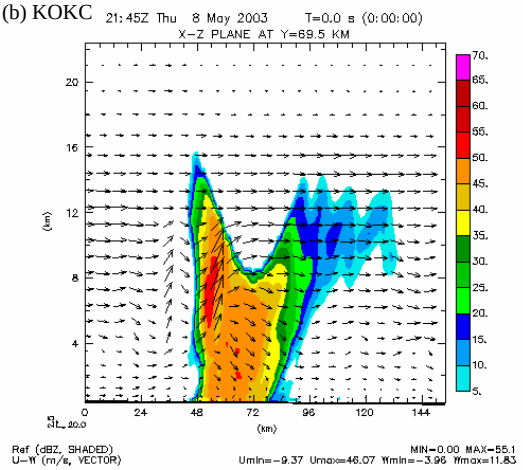

Fig. 4. Cross sections at the location denoted in Fig 3. at 2145 UTC for (a) the control run and (b) the analysis using data from only KOKC.

Other findings from the analysis experiments showed the importance of a three dimensional divergence constraint on eliminating noise and smoothing the analysis (not shown).

4. 1-KM FORECAST RESULTS

Several forecasts were performed at different analysis times and with a varying radius of influence to determine the impact on the forecast.

(a) Control

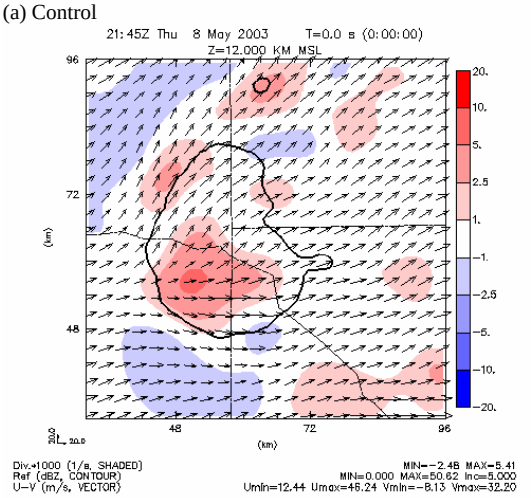

(b) KOKC

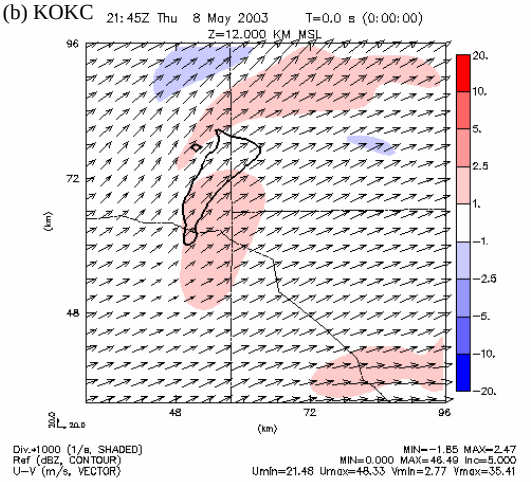

Fig. 5. 12-km divergence and 35dbz reflectivity contours at 2145 UTC for (a) the control run and (b) the analysis using data from only KOKC.

A balanced analysis may be obtained with a radius of influence small enough to resolve the mesocyclone structure while mitigating noise in the wind field that can trigger spurious convection within the unstable and weakly capped environment. During some of the experiments convection formed into a multicell cluster by 2220 UTC. Observations using radar data from this event showed that convection trended towards a multicellular mode until dissipating due to the increase in convective inhibition during the early evening. One of the most successful analyses used as the initial conditions for a forecast was performed at 2155 UTC, which had a minimum radius of influence of 5-km and only included radar data within

the thunderstorm and areas to the southeast within the storm inflow. The development of intense low level rotation at 0.5-km was evident just after 2200 UTC (Shown in Fig. 8b for 2210 UTC) and continued until 2220 UTC when it weakened. The variation of maximum vorticity during this period below the 2-km AGL are shown in Fig. 9 along with the maximum vertical velocity. The peak of maximum vorticity in Fig. 9 coincided roughly with the touchdown time of the actual tornado at 2210 UTC.

(a) Control

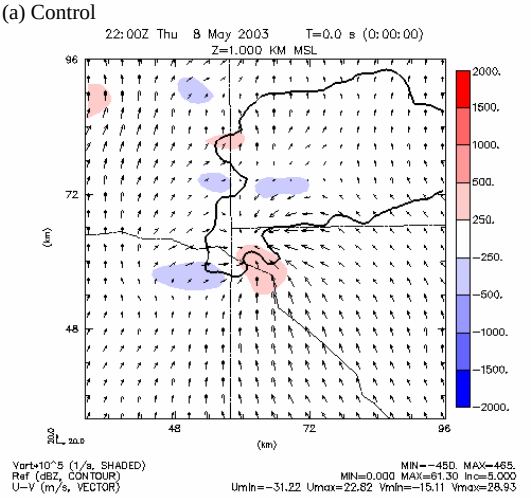

(b) KOKC

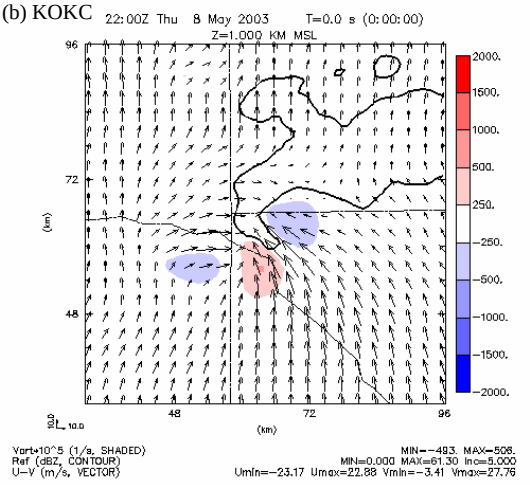

Fig. 6. 1-km vertical vorticity and 35dbz reflectivity contours at 2200 UTC for (a) the control run and (b) the analysis using data from only KOKC.

Although in reality the tornado continued until 2038 UTC, The location of the mesocyclone agreed well with the damage survey (Shown in Fig. 8b) and the analysis performed at 2210 UTC (Shown in Fig. 10) which can be compared to the forecast in Fig. 8a for the same time.

5. CONCLUSION AND FUTURE WORK

The goal of this research was to improve the initial conditions using the 3DVAR analysis technique in hopes of accurately forecasting severe convection on the storm-scale as well as examining the precursors in tornado producing thunderstorms from examining archived data.

In this study the ARPS 3DVAR analysis package was used to create the initial conditions for a forecast of the 8 May 2003 central Oklahoma tornadic supercell. Findings from this study showed that the use data from multiple radars that observe both the lower and upper portions of a convective storm can significantly improve the quality of the analysis by resolving the low level mesocyclone and upper level divergence within the thunderstorm with more detail.

(a) Control

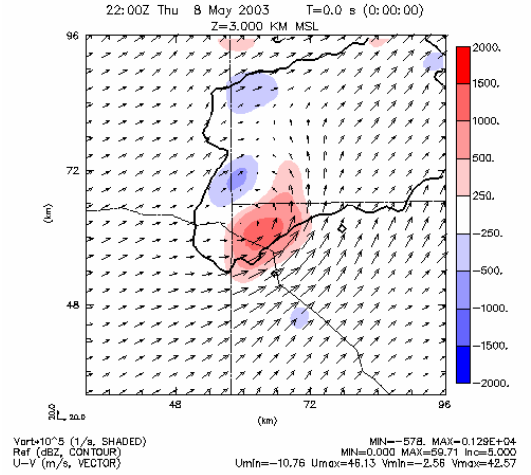

(b) KOKC

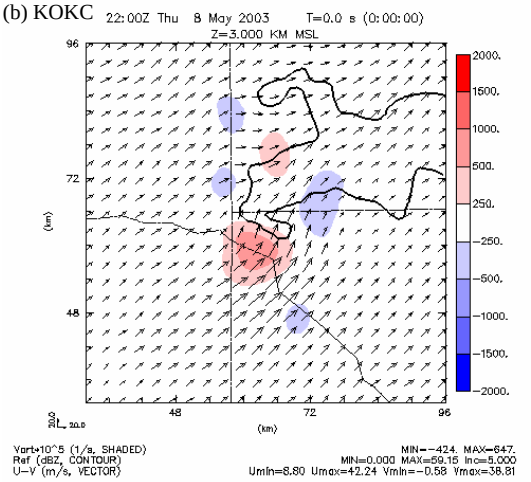

Fig. 7. 3-km vertical vorticity and 35dbz reflectivity contours at 2200 UTC for (a) the control run and (b) the analysis using data from only KOKC.

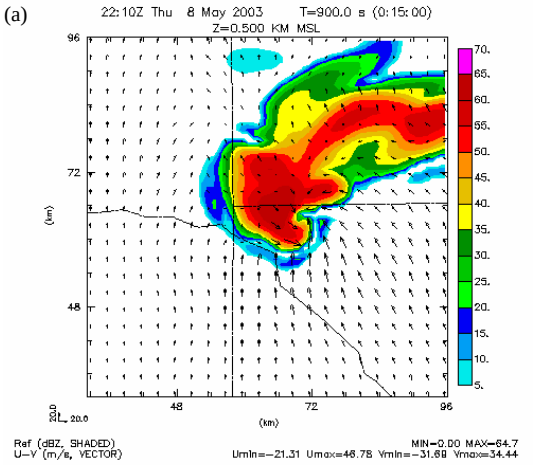

Fig. 8. 0.5-km (a) reflectivity and (b) vertical vorticity and 35dbz reflectivity contours at 2210 UTC for the 1-km forecast. The thick black line (in b) denotes the observed damage path of the actual tornado.

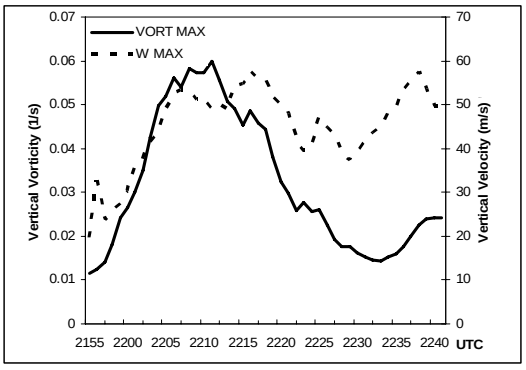

Fig. 9. Maximum vertical vorticity below the 2-km level and maximum vertical velocity for the 1-km forecast.

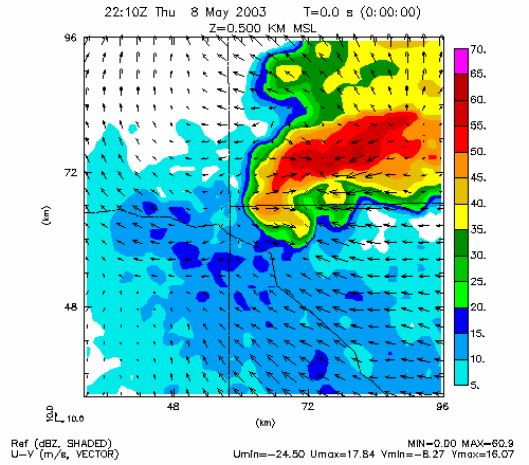

Fig. 10. Observed 0.5-km reflectivity at 2210 UTC from the control analysis.

Using an analysis at 2155 UTC, a 1-km forecast was performed that developed strong low level rotation from 2200–2220 UTC in close proximity to the documented damage path of a F4 tornado in the Oklahoma City area.

Future work includes performing a forecast using an analysis performed at an earlier time, to determine the quality of the initial conditions during convection initiation at 2120 UTC. Other future work includes cycling the model with intermittent 3DVAR analysis at different time intervals. Lastly, to resolve the fine scale structure of the forecast presented in this study, a high resolution forecast will be performed with the same initial conditions but with radar scans interpolated to the exact same time.

REFERENCES

Dowell, D. C., L.J. Wicker, and D. J. Stensrud, 2004: High-resolution analyses of the 8 May 2003 Oklahoma City storm. Part II:EnKF data assimilation and forecast experiments. *Extended Abstract, 22nd Conf. on Severe Local Storms, Hyannis, MA, Amer. Meteor. Soc.*, 12.5

Gao, J., M. Xue, A. Shapiro, Q. Xu, and K. K. Droegemeier, 2001: Three Dimensional Simple Adjoint Velocity Retrievals from Single-Doppler Radar. J. *Atmos. Oceanic Technol.*, **18**, 26–38.

Gao, J., M. Xue, K. Brewster, and K. K. Droegemeier 2004: A Three-dimensional Variational Data Assimilation Method with recursive filter for Single-Doppler Radar, J. *Atmos. Oceanic. Technol*. **21**, 457-469.

Ge, G., J. Gao, 2007: Latest Development of 3DVAR System for ARPS and its Application to a Tornadic Supercell Storm. *Extended Abstract, 18th Conf. on Numerical Weather*

Prediction, Park City, UT, Amer. Meteor. Soc., 2B.6.

Hu, M., M. Xue, and K. Brewster, 2006: 3DVAR and Cloud Analysis with WSR-88D Level-II Data for the Prediction of the Fort Worth, Texas, Tornadic Thunderstorms. Part I: Cloud Analysis and Its Impact. *Mon. Wea. Rev*., **134**, 675–698.

Hu, M., M. Xue, J. Gao, and K. Brewster, 2006: 3DVAR and Cloud Analysis with WSR-88D Level-II Data for the Prediction of the Fort Worth, Texas, Tornadic Thunderstorms. Part II: Impact of Radial Velocity Analysis via 3DVAR. *Mon. Wea. Rev.*, **134**, 699–721.

Hu, M., and M. Xue, 2007: Impact of Configurations of Rapid Intermittent Assimilation of WSR-88D Radar Data for the 8 May 2003 Oklahoma City Tornadic Thunderstorm Case. *Mon. Wea. Rev*., **135**, 507–525.

Hu, M., and M. Xue, 2007: Analysis and Prediction of the 8 May 2993 Oklahoma City Tornadic Thunderstorm and Embedded Tornado using ARPS with Assimilation of WSR-88D Radar Data*. Extended Abstract, 18th Conf. on Numerical Weather Prediction, Park City, UT, Amer. Meteor. Soc.*, 1B.4.

Klemp, J.B., and R.B. Wilhelmson, 1978: Simultions of Right- and Left-Moving Storms Produced Through Storm Splitting. *J. Atmos. Sci.*, **35**, 1097–1110.

Rotunno, R., 1981: On the Evolution of Thunderstorm Rotation. *Mon. Wea. Rev.*, **109**, 577–586.

Sun, J., and N.A. Crook, 1997: Dynamical and Microphysical Retrieval from Doppler Radar Observations Using a Cloud Model and Its Adjoint. Part I: Model Development and Simulated Data Experiments. *J. Atmos. Sci*., **54**, 1642–1661.

Sun, J., and N.A. Crook, 1998: Dynamical and Microphysical Retrieval from Doppler Radar Observations Using a Cloud Model and Its Adjoint. Part II: Retrieval Experiments of an Observed Florida Convective Storm. *J. Atmos. Sci*., **55**, 835–852..

Sun, J., and N.A. Crook, 2001: Real-Time Low-Level Wind and Temperature Analysis Using Single WSR-88D Data. *Wea. Forecasting*, **16**, 117–132.

Wicker, L. J., D. Dowell, 2004:High-resolution analyses of the 8 May 2003 Oklahoma City storm. Part III: An ultra-high resolution forecast experiment. *Extended Abstract, 22nd Conf. on Severe Local Storms, Hyannis, MA, Amer. Meteor. Soc.*, 12.6